https://doi.org/10.1595/205651318X15342609861275 *Johnson Matthey Technol. Rev.*, 2018, **62**, (4), 438–452

JOHNSON MATTHEY
TECHNOLOGY REVIEW

www.technology.matthey.com

Application of Atomic Force Microscopy in Formulation Engineering

A versatile tool for surface analysis

Lawrence Shere and Zhenyu Jason Zhang*
School of Chemical Engineering, University of Birmingham, Edgbaston, Birmingham, B15 2TT, UK

Jon A. Preece
School of Chemistry, University of Birmingham, Edgbaston, Birmingham, B15 2TT, UK

***Email:** z.j.zhang@bham.ac.uk

Atomic force microscopy (AFM) an analytical technique based on probing a surface or interface with a microcantilever, has become widely used in formulation engineering applications such as consumer goods, food and pharmaceutical products. Its application is not limited to imaging surface topography with nanometre spatial resolution, but is also useful for analysing material properties such as adhesion, hardness and surface chemistry. AFM offers unparalleled advantages over other microscopy techniques when studying colloidal systems. The minimum sample preparation requirements, *in situ* observation and flexible operational conditions enable it to act as a versatile platform for surface analysis. In this review we will present some applications of AFM, and discuss how it has developed into a repertoire of techniques for analysing formulated products at the nanoscale under native conditions.

1.Introduction

Formulation engineering (or product engineering) is an approach for developing structural products based on fundamental understanding of the physical, chemical and biological properties of the compounds involved (1, 2). The properties of formulated products such as texture and rheology are determined by the microstructure. However, this correlation is often poorly understood. The formulation engineering approach is used to develop innovative new products with enhanced properties and address challenges such as replacing key product constituents and reducing energy consumption during manufacture. Examples are the development of low fat mayonnaise or the replacement of environmentally harmful chemicals (3, 4).

Despite the wide range of physical instruments available to characterise formulations, very few of them can be used to analyse complex structures at the required submicron resolution. Conventional optical microscopes were limited by the wavelength of light to approximately 200 nm resolution due to the diffraction of light, although the development of super-resolution microscopy has increased the resolution range down to 20–50 nm (5). Electron microscopy techniques, including both transmission electron microscopy (TEM) and scanning electron microscopy (SEM), can interrogate samples with nanometre resolution. However, they generally have to be operated under vacuum conditions and often require a conductive coating on the sample, which causes a significant practical challenge for the development of formulations that are usually liquid based. Other experimental approaches, such as ellipsometry and interferometry, could be used to examine a specific property of the formulation.

Atomic force microscopy (AFM) has become a versatile technique used in various disciplines, ranging from medical research to atom manipulation. AFM can be used to image solid-

liquid or solid-gas interfaces with nanometre lateral resolution and quantify the interfacial forces. AFM belongs to the family of scanning probe microscopy, which includes scanning tunnelling microscopy (STM), scanning near field optical microscopy (SNOM) and magnetic force microscopy (MFM) (6). The first scanning tunnelling microscope was invented in 1981 by Binnig and Rohrer (7, 8), whereby a conducting tip is brought into close proximity with a surface. A tunnelling current is generated by the applied bias between the tip and the surface which is used to control the tip as it scans over the surface, generating a surface topography map. The working principle has since been expanded, utilising various physical parameters (such as electrical field, magnetic field and atomic or molecular interactions) between the tip and the surface to acquire surface properties.

New possibilities of using AFM to interact with samples have been developed which offer a range of advantages over other imaging techniques (9). Because the AFM tip is in direct contact with the sample, it can provide a range of other information regarding the tip-sample interaction and even allows the direct manipulation of the sample at the atomic or molecular level. However, what really puts AFM in a class of its own is that it can perform under a broad range of environments (gas, vacuum or liquid) and does not require any complicated or invasive sample preparation, while the sample can be reused after imaging. This versatility presents opportunities in many scientific and technological areas. It is now very common to see AFM in an industrial setting, due to the importance of nanoscale properties on the success of products. This review aims to demonstrate the burgeoning range of AFM applications in understanding formulations at the nanoscale.

2. Technique

The core component of AFM is a nanoscopic tip mounted on the end of a flexible cantilever (**Figure 1**), most commonly V-shaped or beam-shaped, made from silicon or silicon nitride. The tip is brought into contact with the surface using a piezoelectric actuator ('piezo') (10). Once the sample and the tip are in contact, the piezo moves in the *x* and *y* direction to raster scan over the selected area. During scanning, the cantilever flexes as the tip follows the surface topography, monitored by an optical lever system

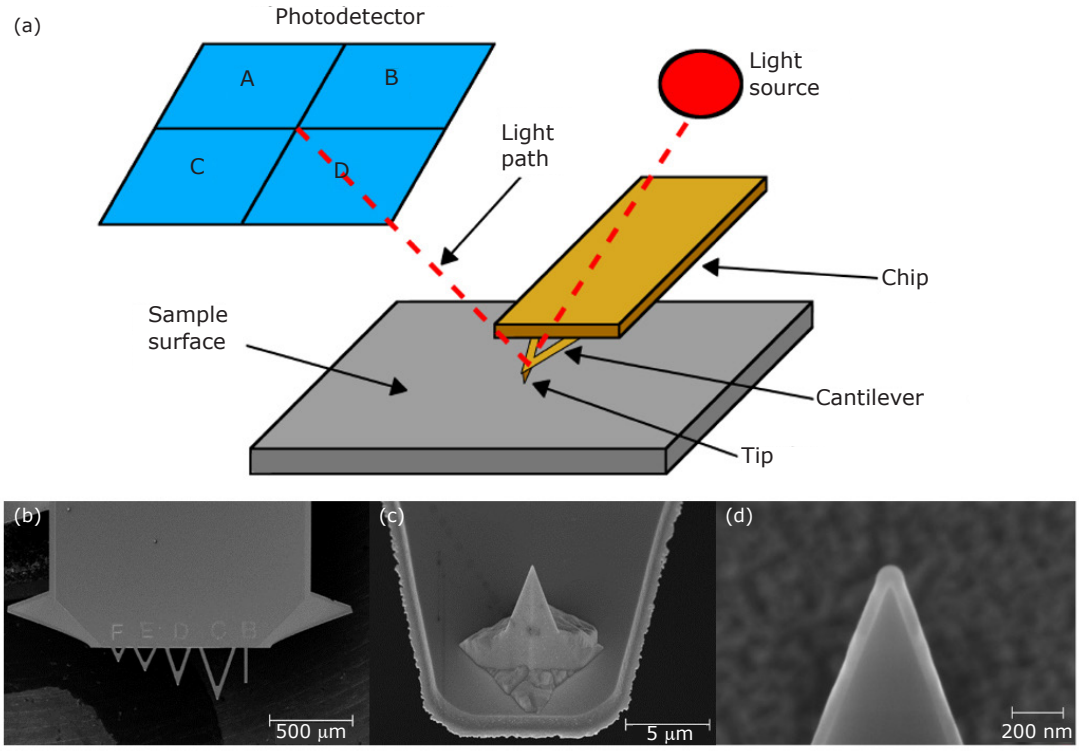

Fig. 1. (a) Schematic diagram describing the operating principle of an AFM. The laser is reflected off the backside of the cantilever (often coated with reflective gold) towards the photodetector. SEM images of AFM chip: (b) with five different cantilevers attached; (c) end of cantilever showing the sharp tip; (d) image of tip

that is composed of a laser source, the reflective backside of the cantilever and a photodetector (**Figure 1**) (11). The photodetector detects the vertical movement and the lateral or torsional bending of the cantilever from the displacement of the reflected laser beam. The deflection of the laser beam amplifies the cantilever deflection angle which is the source of the high sensitivity of AFM. The imaging modes of the AFM can be classified as contact or dynamic modes, depending on the oscillation of the cantilever (12).

2.1 Contact Mode

Contact mode is the simplest and most basic AFM imaging mode, during which the tip is in constant contact with the surface (**Figure 2**) producing a topographical image with nanometre resolution.

As the tip scans across the surface, contact with the surface is maintained by adjusting the vertical position of the cantilever which is controlled by the measured deflection of the cantilever. Contact mode is generally used to image hard samples, or particles that are well adhered onto a surface. It can provide valuable information concerning different frictional properties of a surface from the lateral deflection of the cantilever (13). However, contact mode can cause surface deformation or displacement of molecules or particles chemi- or physisorbed to the surface, due to the force applied by the tip during the scanning process (6). Therefore, when imaging a soft or easily deformable sample, the dynamic modes are preferred.

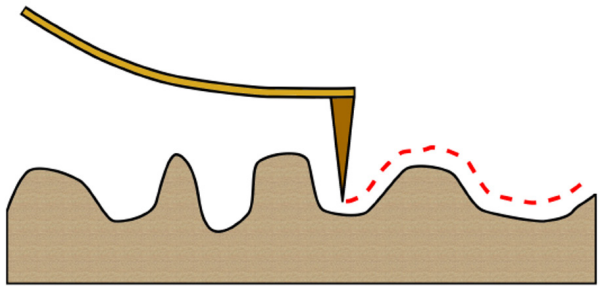

Fig. 2. Graphical representation of AFM imaging with contact mode

2.2 Dynamic Modes

Dynamic modes were developed to address the issues arising from contact mode imaging. In dynamic mode, the cantilever oscillates near its resonance frequency and then is brought into either intermittent contact with the surface or no contact.

- Intermittent contact mode, or amplitude-modulation AFM (AM-AFM): The cantilever oscillates at a set point, periodically contacting and disengaging from the surface at intermittent (or tapping) frequencies (shown in **Figure 3(a)** and **3(b)**). This is one of the most frequently used modes when imaging biological systems due to the minimal sample disturbance and the ability to operate in liquids
- Non-contact mode, or frequency-modulation AFM (FM-AFM): The cantilever oscillates at a reduced amplitude. Instead of making direct contact, the tip interacts with the surface through long range interactions which cause a phase shift between the driving and oscillatory frequencies (shown in **Figure 3(c)**). The advantage of non-contact mode is that surface-tip interactions are minimised. However, this

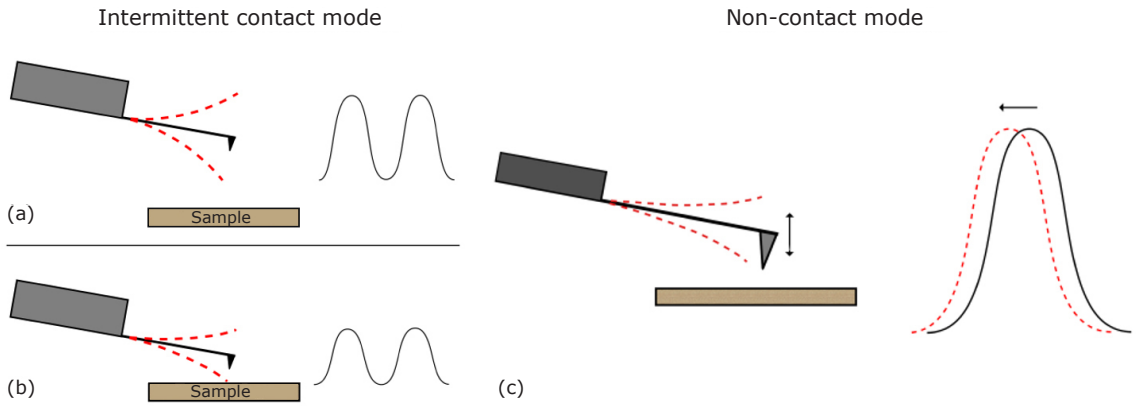

Fig. 3. (a) Intermittent contact mode showing the free oscillation of the cantilever away from the sample near its resonance frequency; (b) when the cantilever approaches the surface its frequency is dampened; (c) non-contact mode. The cantilever is oscillating above the sample near its resonant frequency

is usually only valid in optimal conditions such as in ultrahigh vacuum (UHV), although recent developments in the technique have resulted in liquid imaging with good resolution (14).

Dynamic modes can also provide information regarding the surface properties of a sample by observing the phase shift during scanning. Despite the advantages over contact mode imaging, dynamic mode imaging in liquid can be a challenging task (12). New imaging capacities are being developed, for instance bimodal AFM where the cantilever is excited at several eigenmodes, which allows several material properties such as topography and Young's modulus to be accessed simultaneously (15). AFM has spawned a range of related imaging techniques such as scanning ion conductance microscopy (SICM) and conductance mapping which will be detailed in later sections.

2.2.1 PeakForce Quantitative Nanoscale Mechanical Characterisation

Improvements in AFM equipment in noise reduction, data acquisition and processing speeds have unlocked new possibilities in AFM imaging, including PeakForce Tapping® AFM. This is a relatively new technique developed by the AFM manufacturer Bruker, USA, and is only available on some newer AFM equipment. Its advantages include fast image acquisition and control of the surface engagement force. Similar to tapping mode AFM, the cantilever oscillates in a sinusoidal shape and so is in intermittent contact with the surface, which minimises lateral forces on the sample. It differs from tapping mode because the cantilever oscillation frequency is much lower than the resonant frequency (typical oscillating frequency is 2 kHz) (16). This enables much finer control of the normal force of the tip on the sample because it avoids filtering effects and the dynamics of a resonating system (17).

PeakForce refers to the method used to control the *z*-position of the tip. The AFM system constantly records the forces exerted on the tip during the oscillation. During oscillation of the cantilever, the tip will periodically be in contact with the surface which produces a repulsive contact force. When this force reaches a maximum pre-set trigger value, the controller causes the tip to disengage from the surface. This means that, unlike any standard tapping, with Peakforce Tapping® the maximum force of the tip on the surface can be directly controlled, which is a significant advantage. Additionally, the software extracts a force curve (see Section 2.3) from each oscillation of the cantilever. This can be used to calculate surface nanomechanical properties for each point on the surface and therefore map the adhesion and elastic properties of the surface, at the same time as producing a topographical image.

2.3 Force Spectroscopy

Besides the acquisition of surface images with high resolution, AFM can be used to measure the surface forces with piconewton sensitivity, which provides an insight into the properties of the sample, the tip, or the medium in between. In force spectroscopy measurements, the tip approaches a sample in the normal direction, makes contact and then retracts away from the surface. A representative force curve is shown in **Figure 4(a)**, demonstrating the key features as the tip interacts with the surface.

- At point A, the tip-substrate separation is large with no interaction detected
- During the approaching stage, the tip is

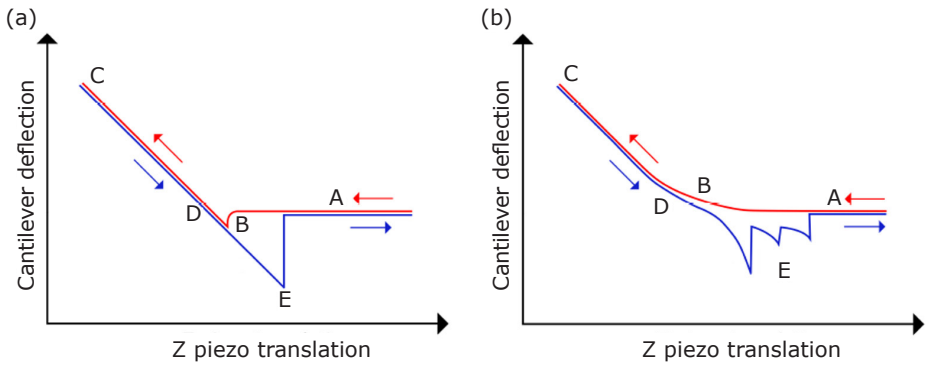

Fig. 4. Schematic representation of force curves. The red line shows the approach of the cantilever towards the surface and the blue line the retraction: (a) idealised force curve for a non-deformable sample exhibiting adhesion; (b) example of force curve against a soft sample exhibiting protein detachment

brought towards the sample (red line) and starts to experience attractive interactions (in close distance) that eventually overcomes the stiffness of the cantilever, which results in a 'jump to contact' event on the surface (point B)
- Between points B–C, the tip is in contact with the surface whilst the cantilever is bent to a certain degree
- From point C, the cantilever withdraws from the surface (blue line). Tip-surface adhesion keeps them in contact (points D–E)
- Eventually, the force induced by the piezo overcomes the tip-surface adhesion and the tip jumps off the surface at point E. The difference between the maximum deflection at E and the baseline at A is quantitatively measured as tip-surface adhesion.

Due to the characteristics of a surface, various force curves can be acquired. **Figure 4(b)** shows a representative force curve collected between a standard tip and a soft sample. An incremental repulsion could be found during the approaching process, which is due to the resistance upon compression by the tip. Multiple peaks could be observed in the retraction part, indicating multiple detachment events. This is characteristic of detaching and unfolding of molecules such as polymers or proteins.

The AFM cantilever, within the operational limits, can be treated as a spring (18). Therefore, the deflection of the cantilever can be translated into force using Hooke's law (Equation (i)):

$$F = kx \quad \text{(i)}$$

where F is the force experienced by the cantilever, k is the spring constant of the cantilever and x is the deflection of the cantilever. Consequently, the z piezo displacement and the cantilever deflection can be converted into sample-tip distance and force by knowing the sensitivity of the laser alignment and the spring constant of the cantilever (19). The nominal spring constant is provided by the manufacturer of the cantilever, but the actual value of the spring constant can vary considerably from the stated value This is due to the strong dependence of the spring constant on the exact thickness of the cantilever. The actual spring constant can be calculated using measurements of the thermal fluctuation of the cantilever (20, 21). Another method, developed by Sader (22), is also routinely used, which uses the measured geometry and resonant frequency of the cantilever in ambient conditions to calculate the spring constant (23).

3. Imaging Soft Matter Interfaces

AFM is compatible with almost any sample, producing images under native conditions. Formulated products are often soft, containing complex mixtures of chemicals, meaning they will be susceptible to damage when using other imaging methods where sample preparation is required. Electron microscopy techniques, for example, require the sample to be imaged under vacuum conditions, causing dehydration and freezing. Super-resolution microscopy requires fluorescent labelling which can lead to bleaching and toxicity (24). For these reasons, AFM imaging could potentially be the most appropriate method to characterise the formulation of a wide range of product types.

Nanostructures in formulations are key to the textural perception of the product and so to consumer satisfaction. When one ingredient in a formulation is replaced by a seemingly very similar ingredient, the consumer experience can be altered radically, for example in eggless cakes. Lin and coworkers (25, 26) investigated the possibility of using pea proteins and plant polysaccharide mixtures as egg substitutes in cakes. AFM images were acquired to evaluate the morphology of glutens in eggless cakes and a conventional egg-containing cake. **Figure 5(a)** shows the structure of glutenin aggregates in a conventional egg-containing cake, in which large pores are observed, indicating an open structure. The authors were able to mimic this porous structure in eggless cake formulations using pea proteins with other additives such as xanthan gum and emulsifiers (shown in **Figures 5(b)** and **5(c)**). These formulations also had similar textures indicating the link between glutenin morphology and macroscale properties. For the eggless cake using only pea protein substitutes, the glutenin appeared to be too compacted to produce any pores. In a similar study, Sow and co-workers (27) used AFM to compare the structure of modified fish gelatine to mimic that of beef gelatine. The diameter of the spherical aggregates and the presence of other nanostructures were found to strongly influence the gelatine texture.

Material characterisation using AFM can be used to highlight changes in the structure and mechanical properties under different conditions. Tapping mode AFM is highly sensitive to changes in material properties such as adhesion and viscoelasticity due to the change in phase lag (28). **Figure 6** shows AFM phase images of carbon fibre reinforced polymer when it is exposed to a 100% relative humidity environment, where the material

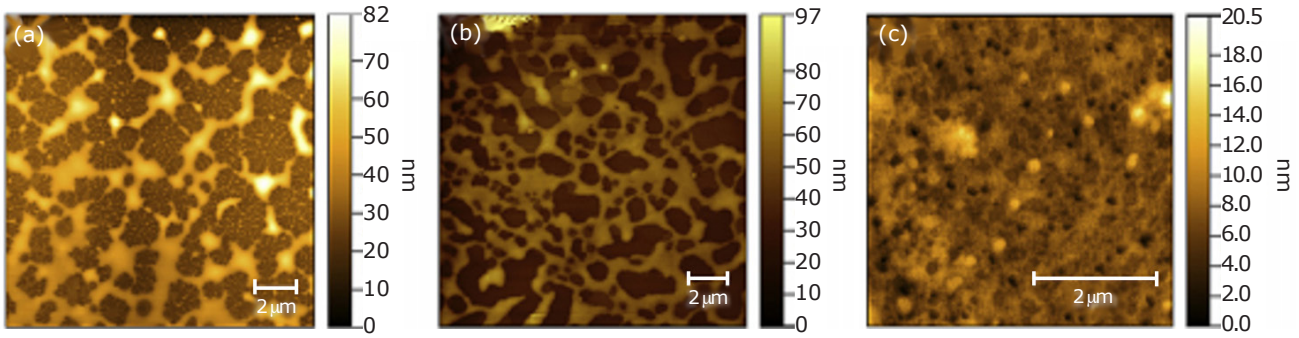

Fig. 5. Glutenin aggregates in: (a) conventional cake; two promising eggless cake formulations with porous glutenin structures using: (b) pea proteins and 0.1% xanthan gum; and (c) pea proteins, 0.1% xanthan gum and 1% mono and diglycerides (MDG). (Reprinted from (25), Copyright (2017), with permission from Elsevier)

structure is changed due to moisture absorption over time. Bright regions in the image demonstrate that the resin is not well bound to the carbon fibres. These changes in structure would be difficult to detect with other methods as the changes are in the local mechanical properties, not topography.

PeakForce Tapping® mode AFM is useful for analysing the microdomains of block copolymers (29–31). It has also been applied to hardened cement paste to quantify the nanomechanical properties of the microphases in the material (16). The researchers analysed the topography, the adhesion force, the sample deformation and the Young's modulus of a 20 µm area of the surface. Four microphases were found on the surface and these were identified using energy-dispersive X-ray spectroscopy (EDX). Using the PeakForce Tapping® AFM data, the researchers were able to quantify the elastic moduli of the four identified phases. Peakforce Tapping® AFM can also be applied to soft surfaces because the force of the tip on the surface can be directly limited in the software to a relatively small value.

In another application, AFM has been used to investigate the dissolution of crystal surfaces. Standard AFM tips can map the change in the crystal surface structure if the kinetics involved are slower than the image acquisition rate (close to equilibrium conditions) (32). Integrated electrochemical AFM (EC-AFM), on the other hand, allows rapid changes in solution concentration and topography to be investigated. This technique uses a conductive platinum coated tip which, through electrolysis, creates a local ion depletion region which creates the driving force for crystal dissociation (33).

A wide range of surface properties can be mapped on the nanoscale using modified AFM tips. For example, by using a conductive metal coated AFM tip, the distribution of surface potential can

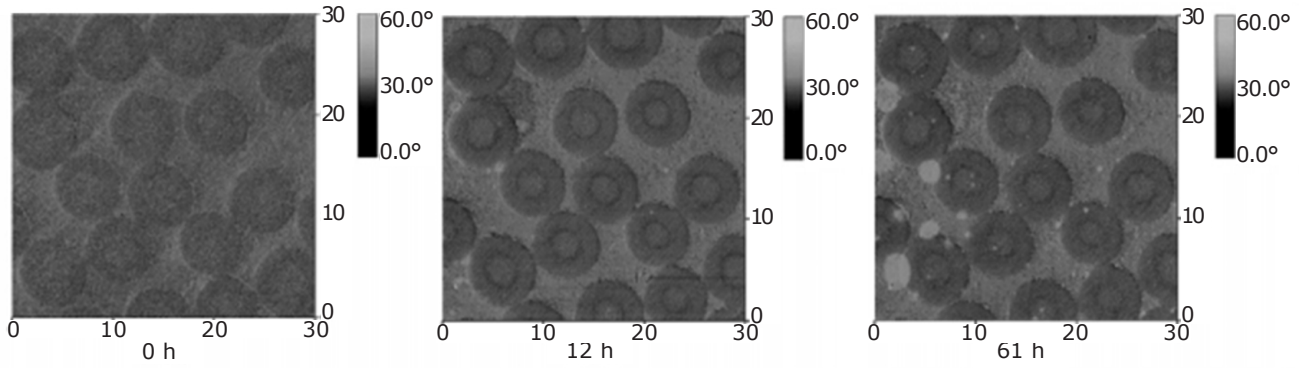

Fig. 6. 30 µm AFM phase images of carbon fibre reinforced polymer samples exposed to 100% RH for different periods of time. The round structures are the carbon fibres showing a typical sheath structure. (Reprinted from (28), Copyright (2007), with permission from Elsevier)

be acquired by applying a potential to the tip. This potential creates an electric force between the tip and charges on the surface (34). This electric force has been used to investigate the static build up on treated and untreated hair surfaces. AFM can also be operated under extreme environments. For example, high temperature AFM has been developed for operation up to 850°C (35). The set-up is the same as a standard AFM but with the sample being tightly attached to a furnace while the piezo is cooled by water flowing through plastic tubes. By applying a sinusoidal alternating current to a conductive tip that scans across the surface, high resolution conductance images of solid oxide cells were collected at 650°C, shown in **Figure 7** (36).

Minimising the force exerted by the tip is a key goal when imaging 'soft' samples because any significant force introduced by the tip will cause deformation and a reduction in resolution. Scanning ion conductance microscopy (SICM) is a non-contact imaging mode developed to overcome this problem. This technique is advantageous for biological systems as the tip does not deform the soft surface or cause contamination (24, 37). This non-contact is achieved by scanning a nanopipette, containing an electrolyte, over the surface whilst monitoring the ohmic resistance between the inside of the pipette and a reference electrode in the bulk solution. As the tip is brought close to the surface, the ionic flow decreases which causes an increase in the resistance. This change in resistance is used to control the tip's position above the surface. **Figure 8** highlights the main differences between SICM and AFM images of fibroblast cells. As well as imaging living cellular systems in an unperturbed state, SICM has also been used for nanoscale studies in electrochemistry and the detection of ions and pH with specialised electrodes (38).

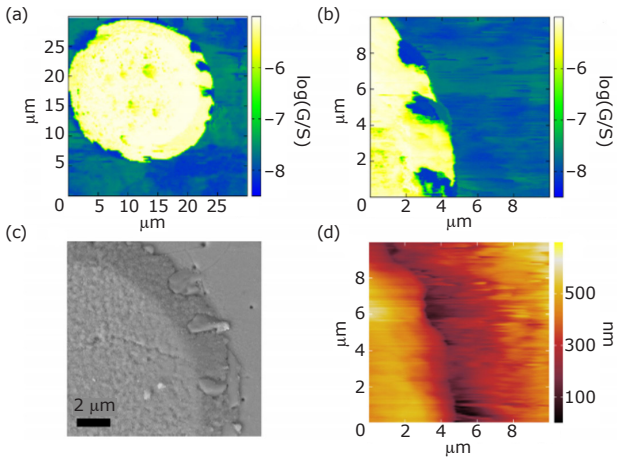

Fig. 7. (a) and (b) Conductance images of a microelectrode obtained at 650°C in air; (c) corresponding SEM image and (d) topography image. (Reprinted from (36), Copyright (2016), with permission from Elsevier)

To establish the distribution of functional groups on a surface, it is possible to use AFM tips that are chemically modified, for example with self-assembled monolayers (SAMs) (39). These tips probe the chemical interactions between the chemically modified tip and the surface functional groups. This technique is referred to as chemical force microscopy (CFM) and it has been used to study surface characteristics of hair fibres (40) and the effect of chemical hair treatment such as bleaching. Using cantilevers functionalised by a methyl terminated SAM, the hydrophobicity of the hair surface was mapped – hydrophobic regions tend to generate strong adhesion. A positively charged ammonium terminated (-NH_3^+) SAM was also used to detect the presence of charged ionic groups on hair (**Figure 9**). This tip was used to map the bleached hair surface which showed highly densely packed ionised cysteic acid (SO_3^-) regions and bare keratin areas of 10–30 nm width.

4. Interfacial Forces

Understanding and quantifying the fundamental forces involved at interfaces is critical for many applications. Experiments at the macroscopic scale have been used for decades to provide useful empirical knowledge. However, the molecular interactions between individual components in a formulation underpin the design and processing of any structural products (41). AFM can be used to establish the local chemical and mechanical properties of a surface. The adhesion force is a key parameter, which can be extracted from AFM force curves (see Section 2.3). For spherical tips (or any well described smooth non-planar geometry), the work of adhesion and the contact area can be calculated from the curvature of the tip and the pull-off force based on contact mechanics considerations, assuming the substrate is smooth and flat, by using elastic deformation models. The models developed by Johnson-Kendall-Roberts (JKR) and Derjaguin-Müller-Toporov (DMT) are commonly used, depending on the system examined. The JKR theory can be used for colloidal tip and soft substrates which exhibit large adhesion (19, 42) (Equation (ii)):

$$F_{ad} = \frac{3\pi RW}{2} \quad \text{(ii)}$$

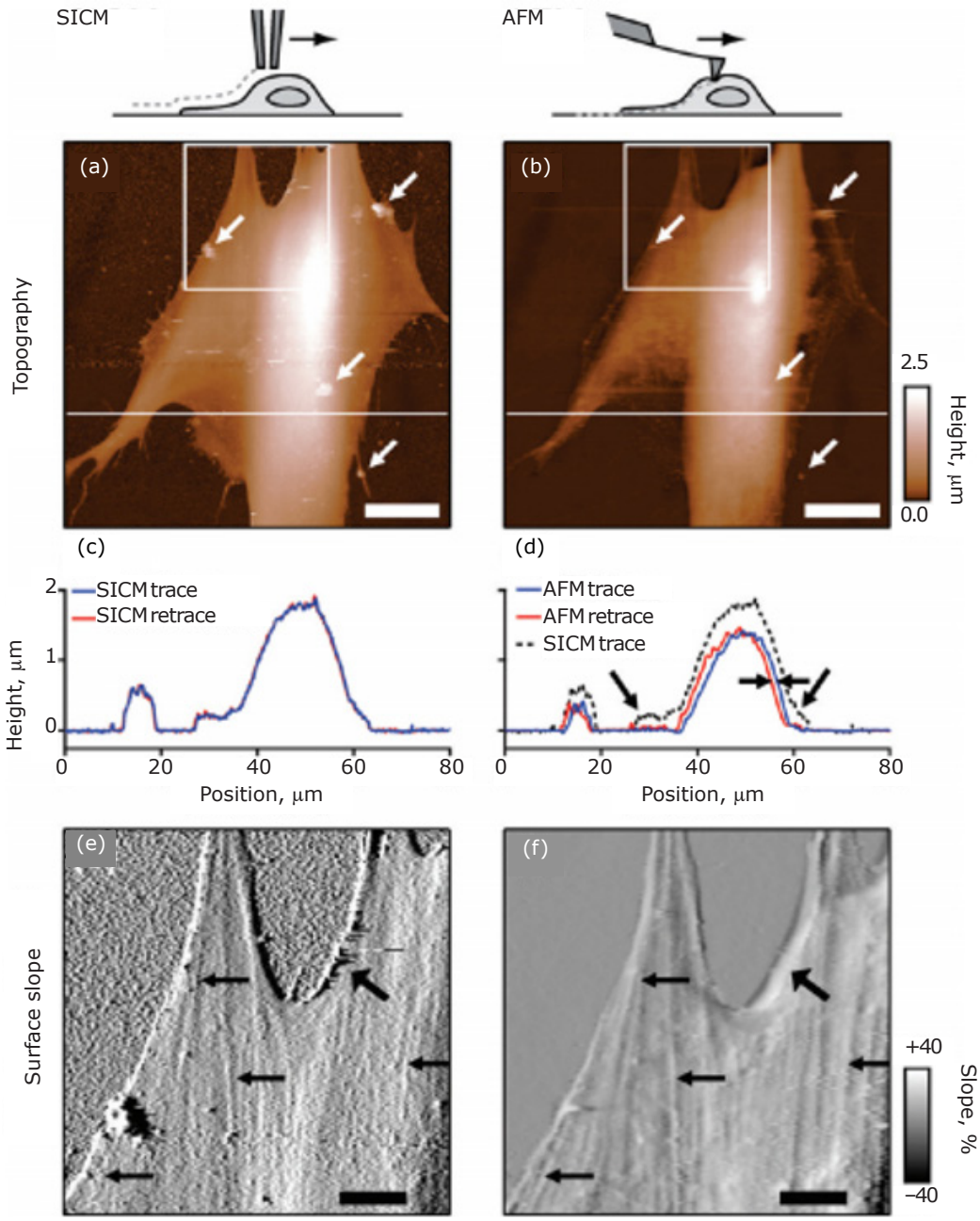

Fig. 8. Comparison of images of the same fixed fibroblast cell taken using: (a) SICM; and (b) tapping mode AFM. Both techniques achieve a similar resolution, however some detail is lost in the AFM image. The cell body also appears much lower in the AFM image as shown more clearly in the corresponding height profiles: (c) SICM and (d) AFM. AFM images on the other hand, show more clearly the fibre-like structure of the underlying cytoskeleton in the zoomed in images shown in: (e) SICM and (f) AFM. (Reprinted with permission from (37). Copyright (2011) American Chemical Society)

where R is the tip radius, W is the work of adhesion per unit area and F_{ad} is the adhesion force. It should be noted that the work of adhesion is directly proportional to the normalised pull-off force (F_{ad}/R) which is valid for whichever contact model is chosen, making it a useful quantity for direct comparison.

The interactions of fine powders with solid surfaces are unpredictable but are of great importance to many industrial processes. AFM has been used in several studies to investigate the forces between single microparticles and solid surfaces (43–47). The colloidal tip technique is a commonly employed variant of AFM which measures the force between a microparticle glued to the cantilever and the surface. This technique is used for a number of reasons (19):

- If the diameter of a smooth microsphere colloidal

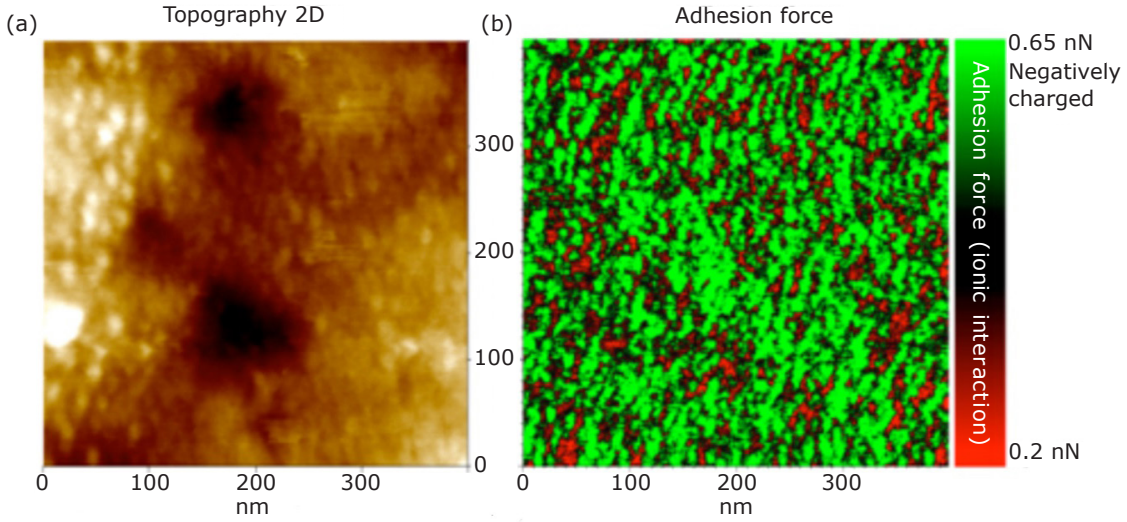

Fig. 9. Fig. 9. (a) Corresponding topography; and (b) adhesion force map (400 nm × 400 nm) of ionic interactions on bleached hair. The image shows two distinct areas with ~80% of the area covered in negatively charged groups (green). (Reprinted with permission from (40). Copyright (2014) American Chemical Society)

particle is known, the force can be analysed quantitatively as the contact area is known
- The total force measured is generally higher due to the increased contact area, which increases the sensitivity of the measurement
- Almost any microparticle (diameter range of 5–50 μm) can be attached to the end of an AFM cantilever enabling this technique to investigate almost any system where particles are involved.

The colloidal tip technique has been used to investigate fouling of equipment during thermal food processing (48). Stainless steel and glass microparticles of 30 μm diameter were glued to AFM cantilevers to produce tips which replicate the surface of the food processing equipment. The adhesion of the colloidal tips to three different food deposits immobilised onto glass slides was measured. The effect of contact time with the surface was investigated. The experiments were conducted at four elevated temperatures by incorporating a heating stage in the AFM. It was predicted that the adhesion force of the fouling deposits would increase with temperature and this was found to be true for whey protein, which denatures and aggregates above *ca.* 75°C, significantly increasing adhesion to all materials tested. For caramel and condensed milk deposits, the greatest adhesion was at low temperatures and long contact times because of the increased material viscosity. In a similar study, Tejedor *et al*. (49) in 2017 used a stainless steel colloidal tip to investigate the mechanism and strength of adhesion of different pharmaceutical powders to metal punches during tableting.

A variety of microscopic objects have been used to produce colloidal tips to model specific systems. Hair fibre cantilevers have been prepared (41, 50) by laser cutting a hair fibre and fixing a fraction to the end of the AFM cantilever with the aid of a micromanipulator. This technique has been further adapted to produce a nanoindenter to investigate how hair fibres interact with skin (50) (**Figure 10**). An ion beam was used to trim the fibre to about 50 μm and produce a cut resembling the effect of a razor-cut facial hair.

Individual emulsion droplets have been attached to an AFM cantilever, enabling direct measurements of the interaction between droplets in the presence of surfactants (51, 52). The AFM cantilever was made hydrophobic following pre-treatment, which allows the cantilever to pick up a droplet that was deposited on a substrate. This droplet tip can then be brought into contact with another droplet on the surface. By relating the forces observed to theoretical analysis (droplet deformation and film drainage), the interplay of forces of stabilisation can be analysed. This analysis can be used to investigate the effect of surfactant concentration in both oil-in-water and water-in-oil emulsion systems.

An understanding of the wettability of rocks and minerals is important for applications such as enhanced oil recovery and froth flotation. However, due to the porosity and heterogeneity of rock surfaces, macroscopic techniques such as contact angle measurements are not always able to

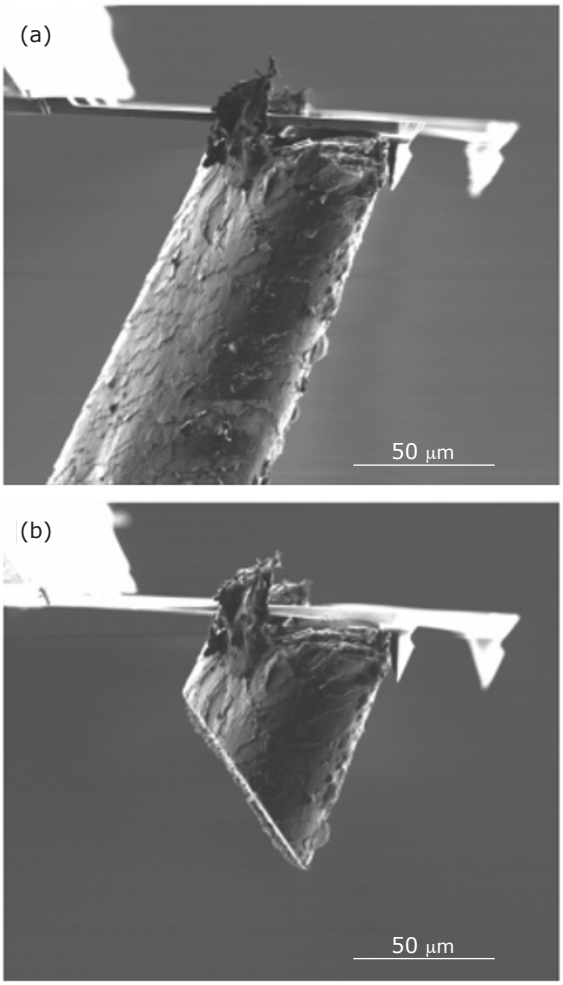

Fig. 10. SEM images of: (a) hair fibre segment vertically attached to AFM tip; and (b) after cutting fibre using ion beam to produce 100 μm long nanoindenter . (Reprinted from (50), Copyright (2016), with permission from Elsevier).

consistently provide quantitative data concerning the surface energy. CFM has been used to probe the adhesion force between mineral surfaces and functionalised tips which mimic the chemical properties of oil in the presence of salt (53–55). This approach has revealed possible mechanisms for the increased water wetting behaviour in low salt conditions. In another study a novel colloidal tip was fabricated to quantify the work of adhesion between calcite surfaces (**Figure 11**) (56). A natural particle was attached to the cantilever and shaped into a smooth hemisphere using a focused ion beam, which ensures a well-defined contact area with flat surfaces for consistent measurements. Xie *et al.* (57) used an AFM tip functionalised with methyl-terminated SAMs to investigate the nanoscale distribution of hydrophilic and hydrophobic domains on sphalerite mineral, after treating with activators and collectors. This analysis revealed a non-uniform distribution of the activator xanthate on the particle surface shown by two distinct hydrophobic and hydrophilic regions.

As well as the tip, the surface of interest must be prepared so it is suitable for AFM. Most real surfaces are highly rough at the nanoscale, making them unsuitable for AFM measurements (58). The surface interactions in lignocellulosic systems are of interest in paper technology. However direct measurements by Neuman *et al.* in 1993 (59) using spin-coated cellulose prepared from dissolved trifluoroacetic acid solution onto mica substrates produced unstable surfaces. Later studies were able to prepare more suitable surfaces using techniques such as Langmuir-Blodgett depositions of trimethylsilyl cellulose on to mica and measuring the surface force between two cellulose spheres. Using these model surfaces the principle short distance surface forces were investigated. Looking at the effect of pH and ionic strength the electrostatic, van der Waals and steric forces could be distinguished. There is still a focus on developing more realistic model cellulose films incorporating the crystallinity of the real surface and the development of novel lignocellulosic materials (58).

5. Polymer Adsorption

AFM is well suited to investigate the adsorption of macromolecules because it is highly surface sensitive and can produce clear images of nanoscale molecular assemblies. Polymers are used in a multitude of applications to modify surface properties of solid-liquid interfaces by adsorbing onto surfaces. Certain polymers are widely used to stabilise colloidal systems by introducing a repulsive force between the particles (60). Adsorbed polymer surfaces are also used to tailor the hydrophobicity of a surface.

AFM can reveal nanoscale structures formed by polymers and proteins on surfaces by mapping the topography, yielding height data related to the swelling of the polymer chains and molecular self-assembly on the surface (61). The adsorption of macromolecules is dependent on a number of factors such as solvent quality and competitive adsorption from other molecules. Therefore, to understand the process, the experimental conditions should be as close as possible to native conditions. Proteins can be covalently bonded to AFM tips through a condensation reaction between amine groups in the protein and carboxylic acid terminated SAM surfaces (62, 63). This enables the molecular interaction between the protein and surface to be

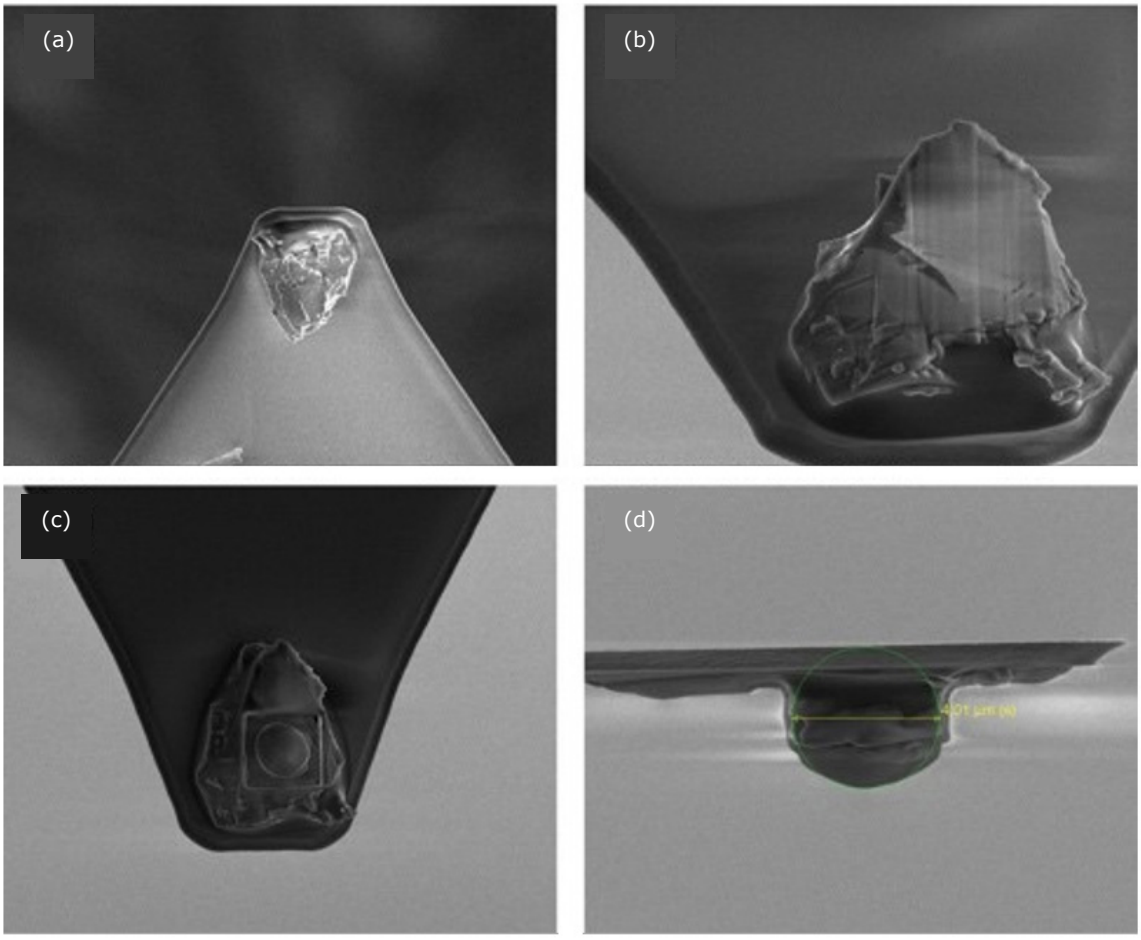

Fig. 11. SEM images of: (a)–(c) calcite particle attached to AFM cantilever, (d) polished and shaped into a 4 μm hemispherical probe. (Reprinted from (56), Copyright (2016), with permission from Elsevier)

probed. Model surfaces utilising SAMs have been used to study specific interactions and tailor the surface wettability (62, 64, 65). Complex surfaces such as polymer substrates can be characterised by high resolution AFM topography images and wettability measurements, enabling the adhesion of proteins to these surfaces to be related to well-defined nanoscale surface properties (63).

Diblock copolymer films, such as polystyrene-*block*-poly(methyl methacrylate) (PS-*b*-PMMA), exhibit microphase separation at the surface because the polymer blocks are immiscible and consequently self-assemble into well-ordered micropatterned domains (66). Many studies have investigated the adsorption of different single proteins to these micropatterned surfaces using AFM imaging (**Figure 12**) (66–69). It was found that some proteins selectively adsorb to a preferred polymer microphase, while the other proteins show concentration-dependent adsorption behaviour. In a study investigating competitive adsorption of two protein species to a diblock copolymer surface, adsorption and displacement processes were observed (69) due to the Vroman effect. Fast-diffusing proteins which initially immobilise on the surface are subsequently replaced by larger proteins that have a slow diffusion coefficient. The nanoscale diblock copolymer surface was found to significantly increase residence time of initially bound proteins when compared to macroscopic uniform polymer surface.

Surfactants and polymers are often used in conjunction to achieve the desired properties in colloidal dispersions. The colloidal tip technique has been used to directly investigate the surface forces in these systems. Sakai *et al.* (70, 71) have investigated the force between alumina surfaces in the presence of anionic surfactant sodium dodecyl sulfate (SDS) and polymers. Addition of only SDS introduces an attractive force between the alumina surfaces, suggesting that the SDS screens the positive charges present on the surface. When SDS was added in conjunction with the non-ionic polymer poly(*N*-vinyl-2-pyrrolidone), the effect of the polymer dominated and so a repulsive force was observed

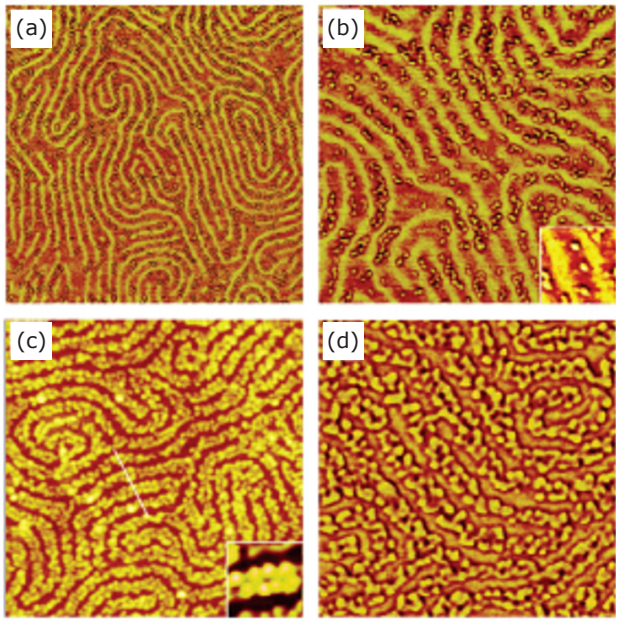

Fig. 12. Selective adsorption of (a)–(b) 4 μg ml^{-1} and (c)–(d) 20 μg ml^{-1} IgG molecules onto preferred polymer microphase on diblock copolymer surface. The images were captured in tapping mode AFM at different scan sizes and imaging modes: (a) 2 x 2 μm phase, (b) 1 x 1 μm phase, (c) 1 x 1 μm topography and (d) 500 x 500 nm phase images. (Reprinted with permission from (66). Copyright (2005) American Chemical Society)

between the surfaces. Liu *et al.* (72) investigated the structures formed by cationic polyelectrolytes and cationic surfactants adsorbing on silica substrates. The authors imaged the micelle structures formed on the surface and used force curves to reveal the time required for the micelle layer to desorb after rinsing, from the disappearance of long range repulsive forces. It was found that the cationic surfactant adsorbed to the surface and formed the same micelle structure, regardless of the presence of the cationic polyelectrolyte or the order of addition.

AFM is also used in many studies to probe the mechanical properties of polymer layers, measuring the friction as the tip is scanned over the surface (73–76). AFM has been used to investigate thermo-responsive polymers in aqueous solutions such as poly(*N*-isopropylacrylamide) by imaging the transition of the polymer structure as the temperature is increased (**Figure 13**) (77). Polymers have also been grafted directly to the silicon nitride surface of AFM tips (78). In another study, a thermo-responsive polymer was grafted onto AFM tips and silicon substrates (79) to assess the effect of nanoscale curvature of the AFM tip on the dynamic polymer brush properties. The curvature of the tip was found to decrease the time required for the polymer layer to swell or contract in response to temperature changes.

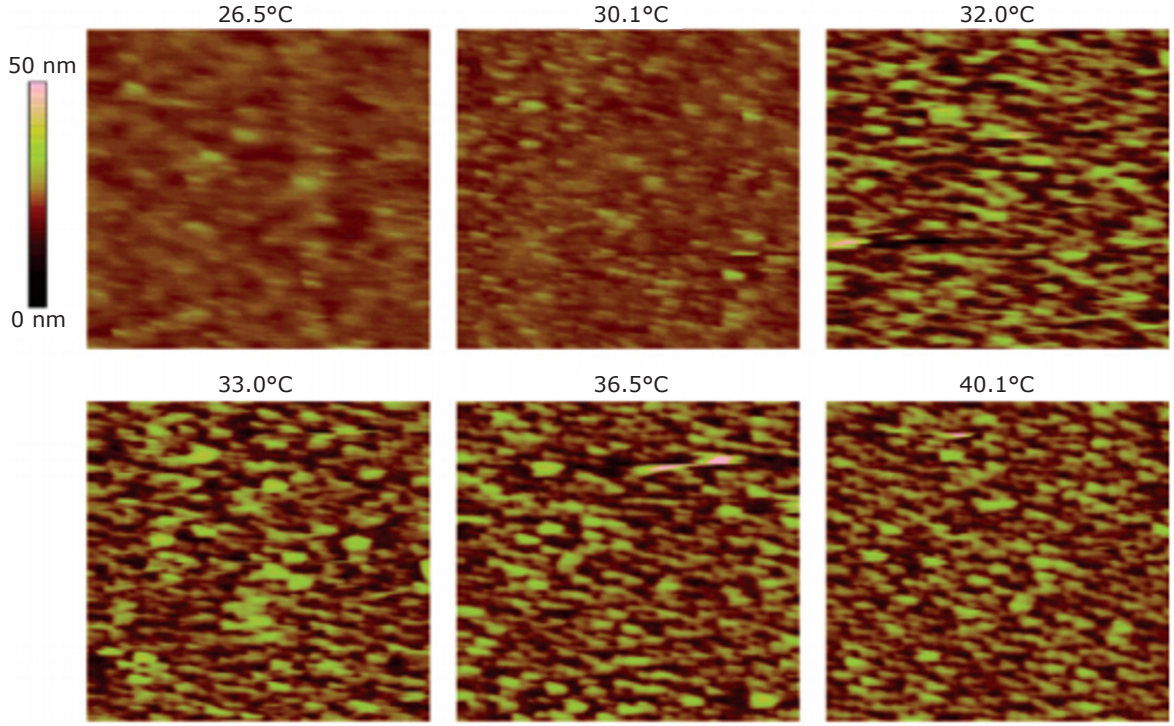

Fig. 13. 2 μm × 2 μm AFM images of poly(N-isopropylacrylamide) layer grafted on silicon. The structure of the polymer layer transitions as the temperature is increased. (Reprinted with permission from (77). Copyright (2007) American Chemical Society)

6. Conclusion

AFM has quickly become a versatile tool for analysing structures and forces from the nanoscale to the microscale. Due to its ability to be used in ambient air or in liquid, most systems relating to formulation engineering can be analysed under native conditions. This versatility has unlocked the ability to assess the effect of process conditions such as humidity and temperature and analyse complex soft formulations such as food and biological samples. New techniques and imaging modes in AFM are being developed, pushing the limits of AFM resolution, precision and scanning speed. The colloidal tip technique has proved to be highly effective at modelling different industrially relevant systems to generate important information about soft matter interfaces. It is a highly adaptable technique with many examples of novel tip design. Although the origins and magnitudes of forces at nanoscale separations are generally well understood, scientists are still in the dark about how these can lead to some of the properties observed in natural systems and products. Using the toolbox of techniques that AFM offers, these systems can be reverse engineered, an approach that is beginning to provide answers to many of these questions.

References

1. H. Schubert, K. Ax and O. Behrend, *Trends Food Sci. Technol*., 2003, **14**, (1–2), 9
2. J. M. Álvarez Gómez and J. M. Rodríguez Patino, *Ind. Eng. Chem. Res*., 2006, **45**, (22), 7510
3. A. L. Ellis, A. B. Norton, T. B. Mills and I. T. Norton, *Food Hydrocoll.*, 2017, **73**, 222
4. J. Santos, L. A. Trujillo-Cayado, N. Calero, M. C. Alfaro and J. Muñoz, *J. Ind. Eng. Chem*., 2016, **36**, 90
5. B. Huang, M. Bates and X. Zhuang, *Annu. Rev. Biochem*., 2009, **78**, (1), 993
6. W. R. Bowen and N. Hilal, "Atomic Force Microscopy in Process Engineering: Introduction to AFM for Improved Processes and Products", Elsevier Ltd, Oxford, UK, 2009, 304 pp
7. G. Binnig, C. F. Quate and Ch. Gerber, *Phys. Rev. Lett*., 1986, **56**, (9), 930
8. G. Binnig, H. Rohrer, Ch. Gerber and E. Weibel, *Appl. Phys. Lett*., 1982, **40**, (2), 178
9. D. P. Allison, N. P. Mortensen, C. J. Sullivan and M. J. Doktycz, *Wiley Interdiscip. Rev.: Nanomed. Nanobiotechnol*., 2010, **2**, (6), 618
10. "Atomic Force Microscopy: Biomedical Methods and Applications", eds. P. C. Braga and D. Ricci, Methods in Molecular Biology Series, Vol. 242, Humana Press Inc, New Jersey, USA, 2004, 394 pp
11. "Atomic Force Microscopy Investigations into Biology: From Cell to Protein", ed. C. L. Frewin, InTech, Rijeka, Croatia, 2012, 354 pp
12. "Atomic Force Microscopy in Liquid: Biological Applications", eds. A. M. Baró and R. G. Reifenberger, Wiley-VCH Verlag and Co KGaA, Weinheim, Germany, 2012, 402 pp
13. C. T. Gibson, G. S. Watson and S. Myhra, *Wear*, 1997, **213**, (1–2), 72
14. T. Fukuma, Y. Ueda, S. Yoshioka and H. Asakawa, *Phys. Rev. Lett*., 2010, **104**, (1), 016101
15. R. Garcia and R. Proksch, *Eur. Polym. J*., 2013, **49**, (8), 1897
16. P. Trtik, J. Kaufmann and U. Volz, *Cement Concrete Res*., 2012, **42**, (1), 215
17. S. B. Kaemmer, 'Introduction to Bruker's ScanAsyst and PeakForce Tapping AFM Technology', Application Note 133, Rev. A0, Bruker Corporation, Santa Barbara, USA, 2011, 12 pp
18. B. Cappella, G. Dietler, *Surf. Sci. Rep.,* 1999, **34** (1), 1
19. H.-J. Butt, B. Cappella and M. Kappl, *Surf. Sci. Rep*., 2005, **59**, (1–6), 1
20. J. L. Hutter and J. Bechhoefer, *Rev. Sci. Instrum*., 1993, **64**, (7), 1868
21. C. M. Franz and A. Taubenberger, 'AFM-Based Single-Cell Force Spectroscopy', in "Atomic Force Microscopy in Liquid: Biological Applications", eds. A. M. Baró and R. G. Reifenberger, Ch. 12, Wiley-VCH Verlag and Co KGaA, Weinheim, Germany, 2012, pp. 307–330
22. J. E. Sader, J. W. M. Chon and P. Mulvaney, *Rev. Sci. Instrum*., 1999, **70**, (10), 3967
23. G. Y. Jing, Jun. Ma and D. P. Yu, *J. Electron Microsc*., 2007, **56**, (1), 21
24. Y. F. Dufrêne, T. Ando, R. Garcia, D. Alsteens, D. Martinez-Martin, A. Engel, C. Gerber and D. J. Müller, *Nature Nanotechnol*., 2017, **12**, (4), 295
25. M. Lin, S. H. Tay, H. Yang, B. Yang and H. Li, *Food Hydrocoll*., 2017, **69**, 440
26. M. Lin, S. H. Tay, H. Yang, B. Yang and H. Li, *Food Chem*., 2017, **229**, 663
27. L. C. Sow, Y. R. Peh, B. N. Pekerti, C. Fu, N. Bansal and H. Yang, *LWT – Food Sci. Technol*., 2017, **85**, (Part A), 137
28. Y. Wang and T. H. Hahn, *Compos. Sci. Technol*., 2007, **67**, (1), 92
29. B. Pollard and M. B. Raschke, *Beilstein J. Nanotechnol*., 2016, **7**, 605
30. M. Lorenzoni, L. Evangelio, S. Verhaeghe, C. Nicolet, C. Navarro and F. Pérez-Murano,

Langmuir, 2015, **31**, (42), 11630

31. L. Cano, D. H. Builes, S. Carrasco-Hernandez, J. Gutierrez and A. Tercjak, *Polym. Test.*, 2017, **57**, 38
32. M. Peruffo, M. M. Mbogoro, M. Adobes-Vidal and P. R. Unwin, *J. Phys. Chem. C*, 2016, **120**, (22), 12100
33. C. E. Jones, J. V. Macpherson and P. R. Unwin, *J. Phys. Chem. B*, 2000, **104**, (10), 2351
34. I. P. Seshadri and B. Bhushan, *J. Colloid Interface Sci.,* 2008, **325**, (2), 580
35. K. V. Hansen, Y. Wu, T. Jacobsen, M. B. Mogensen and L. T. Kuhn, *Rev. Sci. Instrum*., 2013, **84**, (7), 073701
36. K. V. Hansen, K. Norrman and T. Jacobsen, *Ultramicroscopy*, 2016, **170**, 69
37. J. Rheinlaender, N. A. Geisse, R. Proksch and T. E. Schäffer, *Langmuir,* 2011, **27**, (2), 697
38. A. Page, D. Perry and P. R. Unwin, *Proc. Royal Soc. A,* 2017, 473, (2200)
39. D. V. Vezenov, A. Noy and P. Ashby, *J. Adhes. Sci. Technol*., 2005, **19**, (3–5), 313
40. M. Korte, S. Akari, H. Kühn, N. Baghdadli, H. Möhwald and G. S. Luengo, *Langmuir,* 2014, **30**, (41), 12124
41. E. Max, W. Häfner, F. W. Bartels, A. Sugiharto, C. Wood and A. Fery, *Ultramicroscopy*, 2010, **110**, (4), 320
42. S. Gourianova, N. Willenbacher and M. Kutschera, *Langmuir,* 2005, **21**, (12), 5429
43. J. Ally, E. Vittorias, A. Amirfazli, M. Kappl, E. Bonaccurso, C. E. McNamee and H.-J. Butt, *Langmuir,* 2010, **26**, (14), 11797
44. J. Bowen, D. Cheneler, J. W. Andrews, A. R. Avery, Z. Zhang, M. C. L. Ward and M. J. Adams, *Langmuir,* 2011, **27**, (18), 11489
45. M. B. Tejedor, N. Nordgren, M. Schuleit, S. Pazesh, G. Alderborn, A. Millqvist-Fureby and M. W. Rutland, *Langmuir,* 2017, **33**, (4), 920
46. R. Jones, H. M. Pollock, D. Geldart and A. Verlinden-Luts, *Ultramicroscopy*, 2004, **100**, (1–2), 59
47. R. Jones, H. M. Pollock, J. A. S. Cleaver and C. S. Hodges, *Langmuir,* 2002, **18**, (21), 8045
48. K. R Goode, J. Bowen, N. Akhtar, P. T. Robbins and P. J. Fryer, *J. Food Eng*., 2013, **118**, (4), 371
49. M. B. Tejedor, N. Nordgren, M. Schuleit, A. Millqvist-Fureby and M. W. Rutland, *Langmuir,* 2017, **33**, (46), 13180
50. R. Álvarez-Asencio, V. Wallqvist, M. Kjellin, M. W. Rutland, A. Camacho, N. Nordgren and G. S. Luengo, *J. Mech. Behav. Biomed. Mater.,* 2016, **54**, 185
51. S. Mettu, C. Wu and R. R. Dagastine, *J. Colloid Interface Sci*., 2018, **517**, 166
52. C. Shi, L. Zhang, L. Xie, X. Lu, Q. Liu, J. He, C. A. Mantilla, F. G. A. Van den berg and H. Zeng, *Langmuir,* 2017, **33**, (5), 1265
53. J. Wu, F. Liu, G. Chen, X. Wu, D. Ma, Q. Liu, S. Xu, S. Huang, T. Chen, W. Zhang, H. Yang and J. Wang, *Energy Fuels*, 2016, **30**, (1), 273
54. J. Wu, F. Liu, H. Yang, S. Xu, Q. Xie, M. Zhang, T. Chen, G. Hu and J. Wang, *J. Ind. Eng. Chem*., 2017, **56**, 342
55. B. Lorenz, M. Ceccato, M. P. Andersson, S. Dobberschütz, J. D. Rodriguez-Blanco, K. N. Dalby, T. Hassenkam and S. L. S. Stipp, *Energy Fuels*, 2017, **31**, (5), 4670
56. B. Sauerer, M. Stukan, W. Abdallah, M. H. Derkani, M. Fedorov, J. Buiting and Z. J. Zhang, *J. Colloid Interface Sci*., 2016, **472**, 237
57. L. Xie, J. Wang, C. Shi, X. Cui, J. Huang, H. Zhang, Q. Liu, Q. Liu and H. Zeng, *J. Phys. Chem. C.*, 2017, **121**, (10), 5620
58. M. Österberg and J. J. Valle-Delgado, *Curr. Opin. Colloid Interface Sci.*, 2017, **27**, 33
59. R. D. Neuman, J. M. Berg and P. M. Claesson, *Nordic Pulp Paper Res. J*., 1993, **8**, (1), 96
60. M. Turesson, T. Åkesson and J. Forsman, *J. Colloid Interface Sci*., 2009, **329**, (1), 67
61. D. Wang and T. P. Russell, *Macromolecules*, 2018, **51**, (1), 3
62. A. Sethuraman, M. Han, R. S. Kane and G. Belfort, *Langmuir*, 2004, **20**, (18), 7779
63. L.-C. Xu and C. A. Siedlecki, *Biomaterials,* 2007, **28**, (22), 3273
64. S. Kidoaki and T. Matsuda, *Langmuir*, 1999, **15**, (22), 7639
65. W. Zhang, H. Yang, F. Liu, T. Chen, G. Hu, D. Guo, O. Hou, X. Wu, Y. Su and J. Wang, *RSC Adv*., 2017, **7**, (52), 32518
66. N. Kumar and J. Hahm, *Langmuir*, 2005, **21**, (15), 6652
67. N. Kumar, O. Parajuli, A. Gupta and J. Hahm, *Langmuir*, 2008, **24**, (6), 2688
68. S. Song, K. Ravensbergen, A. Alabanza, D. Soldin and J. Hahm, *ACS Nano*, 2014, **8**, (5), 5257
69. S. Song, T. Xie, K. Ravensbergen and J. Hahm, *Nanoscale,* 2016, **8**, (6), 3496
70. K. Sakai, T. Yoshimura and K. Esumi, *Langmuir*, 2003, **19**, (4), 1203
71. K. Sakai, T. Yoshimura and K. Esumi, *Langmuir*, 2002, **18**, (10), 3993
72. J.-F. Liu, G. Min and W. A. Ducker, *Langmuir*, 2001, **17**, (16), 4895
73. J. An, X. Liu, A. Dedinaite, E. Korchagina, F. M. Winnik and P. M. Claesson, *J. Colloid Interface Sci*., 2017, **487**, 88

74. A. Raj, M. Wang, C. Liu, L. Ali, N. G. Karlsson, P. M. Claesson and A. Dėdinaitė, *J. Colloid Interface Sci*., 2017, **495**, 200
75. A. Naderi, J. Iruthayaraj, T. Pettersson, R. Makuška and P. M. Claesson, *Langmuir*, 2008, **24**, (13), 6676
76. N. Nordgren and M. W. Rutland, *Nano Lett*., 2009, **9**, (8), 2984
77. N. Ishida and S. Biggs, *Langmuir*, 2007, **23**, (22), 11083
78. S. Gabriel, C. Jérôme, R. Jérôme, C.-A. Fustin, A. Pallandre, J. Plain, A. M. Jonas and A.-S. Duwez, *J. Am. Chem. Soc*., 2007, **129**, (27), 8410
79. N. Willet, S. Gabriel, C. Jérôme, F. E. Du Prez, A.-S. Duwez, *Soft Matter*., 2014, **10**, (37), 7256

The Authors

Lawrence Shere graduated from the University of Bimingham, UK, in 2016 with a Masters degree in Chemical Engineering. He is now conducting a PhD at the same university, sponsored by Innospec Inc, USA, to develop a 'bottom-up' approach to design speciality chemicals. His project concerns soft matter at the solid/liquid interface where molecular interactions and interfacial conformation are critical.

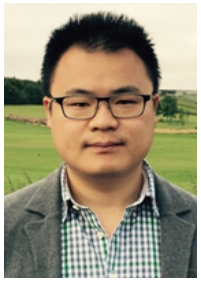

Zhenyu Jason Zhang is a Lecturer at the School of Chemical Engineering, University of Birmingham. He holds a PhD degree in Polymer Physics and has over 15 years' experience and expertise in soft matter and nanotribology with engineering and biomedical applications. Polymer and colloids at interfaces, including their adsorption kinetics, frictional and adhesive properties and response to external stimuli, is a key theme of his work. His group has broad activities in both formulation engineering and bio-applications, which are or have been supported by EPSRC, Medical Research Council (MRC), the Royal Academy of Engineering, the Royal Society, the Carnegie Trust, Energy Technology Partnership, European Cooperation in Science and Technology (COST) Action and industrial partners including Procter & Gamble, Schlumberger and DuPont Teijin Films.

Jon A. Preece began his academic research career in the Group of Professor J. Fraser Stoddart, University of Birmingham (1991–1994) carrying out research in the area of supramolecular chemistry, with particular interest in the design, synthesis and characterisation of materials which could be switched between different states. This interest in materials chemistry led Preece to join the Research Group of Professor Helmut Ringsdorf, Johannes Gutenberg University, Mainz, Germany, for a period of two years (1995–1996) where he gained experience in aspects of materials surface science. Currently, the Preece Group carries out research in the area of nanoscale materials science. For example, new nanoscale-materials: (i) for electron beam resists; (ii) for the assembly of inorganic/organic hybrid nanoparticles with novel electro-optic, structural and medicinal properties (gene delivery); (iii) for liquid crystals; and (iv) for surfaces used in technological applications. The research is or has been supported by the Engineering and Physical Sciences Research Council (EPSRC), Biotechnology and Biological Sciences Research Council (BBSRC), European Community (Research Training Network (RTN), Specific Targeted Research Projects (STREP)), The Leverhulme Trust and New Energy and Industrial Technology Development Organization (NEDO), Japan, as well as two leading British companies (BAE Systems and British Nuclear Fuels Ltd (BNFL)).